Full Paper: In this paper we want to report the results obtained in our study of the cold-crystallization kinetics of PPS samples quenched from the melt state and analyzed in the crystallization temperature range 90–112 °C. Such a wide range was explored by employing three different experimental techniques: the first one was the usual Differential Scanning Calorimetry (DSC), for the highest temperature range, the second and third ones were the less conventional FT-IR spectroscopy and energy dispersive X-ray diffraction (EDXD), able to explore the lowest temperature range. The experimental data obtained by the three above mentioned methods have been all together analyzed by means of the Avrami equation. FT-IR and EDXD have also allowed us to study the secondary crystallization process of PPS, which otherwise could not be observed just with the DSC technique. The overall crystallization process of such a polymer has been interpreted in the light of the model proposed by Ravindranath and Jog to explain the crystallization of the polymer from the melt state.

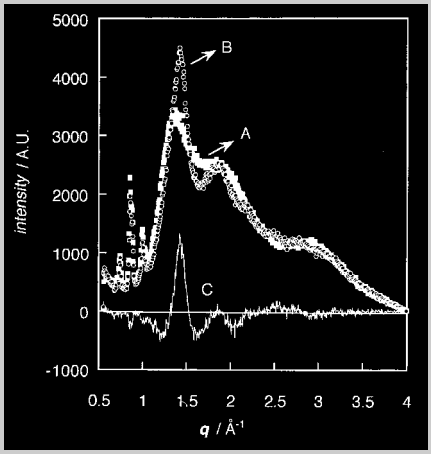

EDXD diffraction spectra of PPS (T_c = 100 °C) measured at 100 °C, t = 0 (A), t = 6600 s (B) and their difference B-A (C).

Poly(*p*-phenylene sulfide) Isothermal Cold Crystallization Investigated by Usual and Unusual Methods

Ruggero Caminiti,[1] *Lucio D'Ilario,**[2] *Andrea Martinelli,*[2] *Antonella Piozzi*[2]

[1] Dipartimento di Chimica, Istituto Nazionale per la Fisica della Materia, Università di Roma "La Sapienza", PO BOX 34 – ROMA 62, Roma, Italy
[2] Dipartimento di Chimica, Università di Roma "La Sapienza", PO BOX 34 – ROMA 62, Roma, Italy
Fax: +39-06-49913740; E-mail: lucio.dilario@uniroma1.it

Introduction

The crystallization kinetics of polymers may be followed both from the melt state and, if their glass transition temperature is not too low, from the solid amorphous one on samples rapidly quenched. In the latter case the crystallization process is diffusion controlled and is commonly known as cold-crystallization. In general the degree of crystallinity which may be achieved in the cold-crystallization experiments is not very high as well as the crystallization enthalpy involved. In such a case it is very difficult, and in some cases rather impossible, to follow the crystallization process by means of the Differential Scanning Calorimetry (DSC), usually employed for this kind of investigation, because of the signal output noise due to the calorimeter sensitivity. Moreover, the high crystallization rate may induce non-isothermal crystallization during the thermal stabilization of the calorimeter or during the sample heating. All these problems often make the DSC temperature range, in which it is possible to collect reliable experimental data to verify theories, rather small.

All the above mentioned reasons make polymers with high glass transition temperature and high crystallization temperature the more suitable to investigate the cold-crystallization process, which may be followed at a temperature higher than room temperature. One of these is the poly(*p*-phenylene sulfide) (PPS), for which a T_g near to 68 °C has been found in experiments done at low heating rate[1] (0.1 °C · min^{-1}).

While the melt-crystallization of PPS has been the object of a large number of studies,[2–15] the cold-crystallization phenomenon does not seem to be equally well treated,[2, 4–7, 9, 13, 14] probably for the above mentioned rea-

  1022-1352/2001/1410–2902$17.50+.50/0

sons. It follows that the theoretical framework describing the crystallization of polymers may not be considered completely consolidated.

The differences in the experimental procedures employed for such studies (dwelling time and temperature of the polymer in the melt state before the start of the crystallization process) and in the chemical nature of the materials (molecular weight, polydispersity, chemical nature of the endgroup counter atom, branching) may explain the wide range of variability of the rate constant k of the melt-crystallization process and of the exponent n of the Avrami law, largely used to explain the experimental data. In the case of PPS n has been found to vary between 2.0 and 3.1, and quite seldom this value is given for the cold-crystallization process. Huo and Cebe[16] quote a 2.9 figure obtained at 110 °C by means of a dielectric relaxation experiment. Maffezzuoli et al.[7] have found n values between 1.91 and 2.37 for amorphous samples of as received PPS neat resin and between 1.55 and 1.81 for PPS reinforced with carbon fibre.

Usually, in order to describe the crystallization kinetics (melt- and cold- crystallization) it is preferred to consider the half-crystallization time $t_{1/2}$. This may be obtained from the Avrami equation, as function of the crystallization temperature T_c.[2, 15] In the first papers[2, 4] in which such an analysis was employed, the experimental data were fitted by means of a second or third order polynomial and the T_c corresponding to the maximum crystallization rate was extrapolated (for PPS a value of about 180 °C was found). To avoid the problems connected to the crystallization start detection, one could also consider the time corresponding to the maximum transformation rate t_{peak}[6, 14] directly determined from the exothermal DSC peak. The possibility of making an interpolation of the kinetic data with a single function was argued by Chung and Cebe[6] which found a different dependence of the crystallization rate on T_c when identified by t_{peak}. These authors have made the hypothesis that the short-range ordered structure in the amorphous solid material, obtained through the quenching procedure, may be responsible for the presence of crystallization nuclei and then of the higher overall cold-crystallization rate compared to the melt-crystallization process. Indeed Ferrara et al.[17] have measured a 10% (w/w) residual crystallinity in quenched PPS samples by considering the difference between the crystallization and the melting ΔH. On the other hand Wu et al.[14] have shown that a symmetrical curve of the t_{peak} as function of T_c is obtained, indicating the non-existence of two different nucleation mechanisms for the melt- and the cold-crystallization.

Lovinger et al.,[3] by studying PPS samples from which traces of ionic by-products of polymerization reaction had been removed by water extraction in order to minimize the high nucleation rate, have shown different behaviors of PPS as function of the isothermal crystallization temperature by measuring the growth rate G in optical microscopy experiments carried out in a wide range of undercooling conditions. In fact, they found a transition in the linear spherulitic growth rate from the crystallization regime III to II at about 208 °C in the case of an intermediate molecular weight PPS (MW 51 000).

As far as the secondary crystallization process of PPS is concerned it was analyzed by a number of authors. Ravindranath and Jog[10] have tried to interpret the fractional n Avrami values found in melt-crystallization experiments by means of the established theories and by means of a new theoretical model which they proposed. Woo and Chen[12] have proposed a series-parallel crystallization model based on modified Avrami equation to interpret their own secondary crystallization experiments on solvent-treated PPS with traces of α-chloronaphthalene. Cole et al.[18] have indirectly made the hypothesis of the presence of secondary crystallization processes by studying the isothermal annealing of PPS Ryton AC40-60 reinforced with carbon fibers in experiments carried out for one hour in the temperature range 105–180 °C. Subsequently also Chung and Cebe[6] have observed such a phenomenon on quenched samples annealed for one hour in the temperature range 140–265 °C.

In this paper we want to report our results on the kinetics of the cold-crystallization of PPS samples quenched from the melt state obtained in a wide range of crystallization temperature (90–112 °C). We have been able to make this investigation by using three different experimental techniques: first the usual DSC, by which we have explored the highest temperature range, second and third the less conventional FT-IR spectroscopy and energy dispersive X-ray diffraction (EDXD),[19] able to explore the lowest temperature for which the transformation is particularly slow. The experimental data obtained by the three above mentioned techniques have been all together analyzed by means of the Avrami equation. FT-IR and EDXD have also allowed us to study the secondary crystallization process of PPS, which otherwise could hardly be observed with just the DSC technique. To explain the crystallization of PPS from the solid amorphous state we have interpreted our overall crystallization results in the light of the model proposed by Ravindranath and Jog.[10]

Experimental Part

PPS Ryton V-I powder ($\overline{M}_w$ = 14 000) from Phillips Petroleum was purified from low molecular weight components by a previous treatment in Soxhlet column with tetrahydrofuran. All the cold-crystallization experiments were carried out by heating at 300 °C for 40 min and then quenching the polymer in liquid nitrogen. Preliminary experiments on the PPS melt-crystallization kinetic were carried out in order to chose the temperature over T_m and the dwell time in the melt state so as to ensure an optimal rearrangement of the polymer

chains, allowing the best loss of the order characterizing the original crystalline phase. Changes of the chemical nature of the polymer (cross-linking, degradation, etc.) that can occur during this procedure, if present, are of minor entity and do not modify neither the IR spectra nor the final crystalline structure of the polymer, as found in WAXD experiments, nor the polymer solubility in diphenyl ether.

The DSC measurements were accomplished by means of the Mettler TA3000 instrument, equipped with a silver furnace. Isothermal cold crystallization experiments were carried out by heating about 8 mg of quenched sample at a rate of 100 °C · min^{-1} from 23 °C to the crystallization temperature in the range 108–112 °C. All the measurements were carried out under N_2 flow.

IR spectroscopical measurements were carried out on a Mattson Galaxy 5020 FT-IR instrument working at 1 cm^{-1} resolution. In order to make sure the accuracy of the samples thermal treatment all the experiments were accomplished by dispersing the polymer powder in KBr disks, which were, as in the case of the other experiments, first heated at 300 °C for 40 min and then quenched in liquid nitrogen. The amorphous content of the samples was by this way maximized. The measurements were accomplished in air, being negligible the CO_2 and H_2O contribution to the absorption peaks analyzed in the present work. The isothermal cold-crystallization was carried out by heating amorphous (quenched) samples at a temperature in the range 90–105 °C, using the Variable Temperature Cell Specac P/N 21525, working in the range −150 to 250 °C, driven by a Hellma P/N 830004 temperature controller. During spectral recording the temperature was kept constant within ±1 °C. The number of interferograms accumulated for each spectrum was 50, at a resolution of 1 cm^{-1}. The temperature was controlled by means of a K-type thermocouple held in physical contact with the KBr disk.

The PPS samples for the EDXD experiments were prepared according to the above mentioned procedure by heating about 200 mg of polymer at 300 °C for 40 min. They were then quenched in liquid nitrogen. To maximize the rate of heat exchange during measurements the samples were supported on copper frame. The great distance of the inner edge of the frame from the X-ray beam compared to the small spherulites size and the small mass ratio between the polymer on the surface in contact with the copper frame and that on the bulk of the sample exclude any influence of the metal on the crystallization process. Sample thickness was about 2 mm. The same temperature cell used for the IR experiments was employed. The sample temperature was recorded with a K-type thermocouple held in physical contact with the polymer. Isothermal crystallization was achieved by rapidly heating the sample at temperature of 95 and 100 °C and spectra were recorded for 10 h.

The diffraction experiments were carried out by employing an X-ray energy scanning diffractometer which was described in previous papers.[1, 19] Our experiments were performed in transmission geometry. Each spectrum was measured for 500 seconds. Oxidation and chemical chain rearrangement effects, occurring in sample preparation and subsequent heating experiment, were excluded by infrared spectroscopy analysis. The amorphous structure of the as-prepared samples was checked before each experimental measurement by verifying the absence of Bragg reflections in angular dispersion X-ray diffraction experiments and comparing their EDXD spectrum to that of a melt crystallized non-quenched sample. These spectra were obtained at room temperature.

Results and Discussion

Primary Crystallization

FT-IR Analysis

The infrared spectrum of the amorphous PPS is affected during heating by more or less pronounced variations. In a previous paper[1] we have already discussed these findings observed across the glass transition temperature region of the polymer. These variations were observed in particular for some absorptions and resulted to be quite small. An inflection of the peak intensity slope as function of temperature in correspondence of T_g was the most evident effect. Such a behavior was attributed to small conformational changes and small amplitude libration of the phenyl rings that affect the resonance of sulfur electrons with the aromatic system, leading to a change in the electron delocalization and modification of the dipolar momentum or to the relaxation of internal stresses caused to the chain by the quenching process. At higher temperature the PPS spectrum shows, in correspondence of the crystallization phenomenon, marked modifications reflecting the chain reorganization process through substantial conformational rearrangements and effects due to the packing of nearby chains. The main differences in the PPS spectra corresponding to the amorphous and to the crystalline states were reported in the early work of Brady[20] and later on by Piaggio et al.,[21] Cole et al.[18] and Zimmerman et al.[22]

Figure 1 shows the quenched PPS (high amorphous content) spectrum (A) and that of an annealed (high crystalline content) sample (9000 s at 98 °C) (B) as well as the one to one subtraction of spectrum B minus spectrum A (C).

As it was pointed out by Zimmerman et al.,[22] the crystallization process due to the heating of the solid amorphous polymer gives rise to a substantial change of the infrared spectrum of PPS, affecting differently nearly all the absorbance peaks. Some of them markedly decrease (1568 and 1473 cm^{-1}) or increase (819 and 825 cm^{-1}), being directly associated to the amorphous and the crystalline phase of the polymer. Some others show a more complicated modification, evidenced by the derivative-like appearance of the signals in the difference spectrum. This is what happens for the absorptions at 1385, 1091, 1072, 1009, and 483 cm^{-1}, affected by small wavelength shifts of the peak center or by their shape variation.

In Table 1 the most important assignments after Zimmerman et al.[22] are reported.

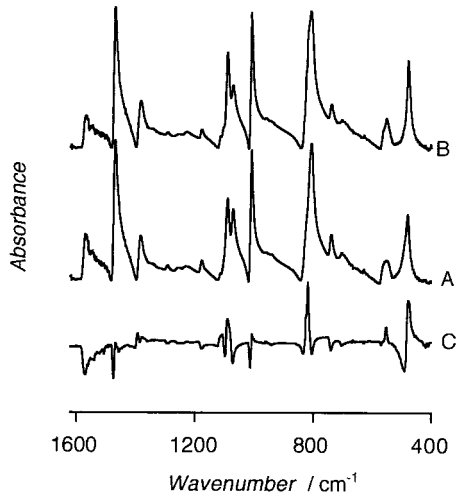

Figure 1. FT-IR spectra of PPS (T_c = 98 °C) recorded at t = 0 (A), t = 9000 s (B) and their difference B-A (C).

Table 1. Main infrared band assignments of PPS according to Zimmerman.[22]

Peak position / cm^{-1}	Band assignment
1570	
1470	Ring stretching
1380	
1091	Anti. ring-S stretching
1072	Sym. ring-S stretching
1009	C—H i. p. deformation
809	C—H o. p. deformation
740	Ring deformation
481	o. p. skeletal deformation

The different crystallization processes, carried out at different temperature, were followed by recording the peak intensities as function of time. In order to compare the spectra evolution of the different experiments, in Figure 2 the values of the absorbance ratio R between the bands at 1092 and 1072 cm^{-1}, which is a measure of the relative crystallinity of the polymer are reported as function of t. These absorptions are sensitive, as stated by Cole et al.,[18] to the crystalline and amorphous phase content of the polymer. For seek of clarity only some T_c were reported in Figure 2. The differences of the R value at the end of the experiments are due to the different crystallinity reached by the polymer at the different crystallization temperature, and not, as we have verified, to the effect of the different sample temperature on the spectrum, which affects R of about +0.2% · °C^{-1}.

The Figure clearly shows that, after a sudden crystallinity increase due to the primary crystallization process, R does not level off, and on the contrary continues to grow with time for a secondary crystallization phenomenon which will be discussed later on.

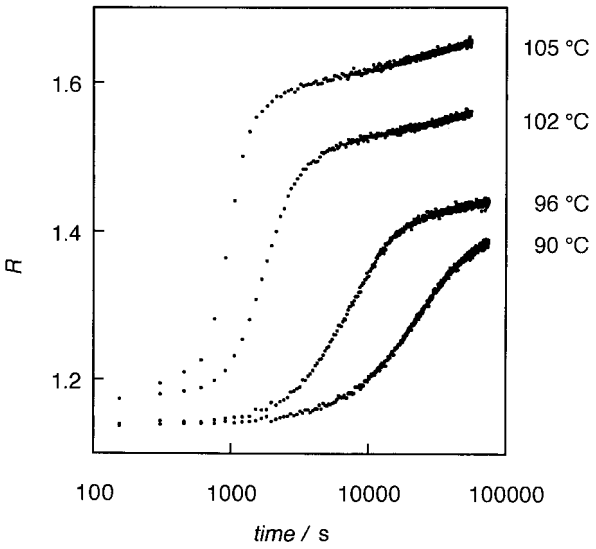

Figure 2. Absorbance ratio R = Abs_{1091}/Abs_{1072} as a function of crystallization time for different T_c.

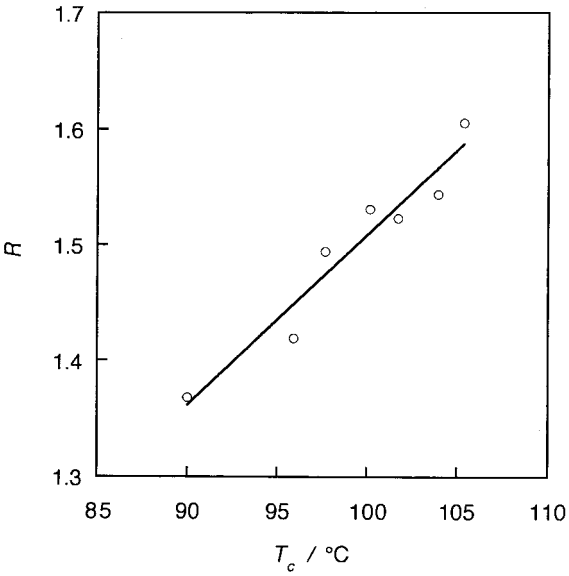

Figure 3. Absorbance ratio R = Abs_{1091}/Abs_{1072} as function of T_c after 15 h of isothermal crystallization.

Figure 3 shows the R variation after 15 h as function of T_c.

The relative crystallinity reached by the polymer in the annealing time and temperature range explored grows linearly with T_c, although the maximum value observed (R_{max} = 1.62) is much lower than that of a PPS sample crystallized by dilute solution (R = 2.4).

In order to give a quantitative description of the polymer crystallization kinetic we have studied the correlation between the crystallinity variation during the isothermal crystallization process and the increase of the two crystalline bands at 819 and 825 cm^{-1}, associated to interchain

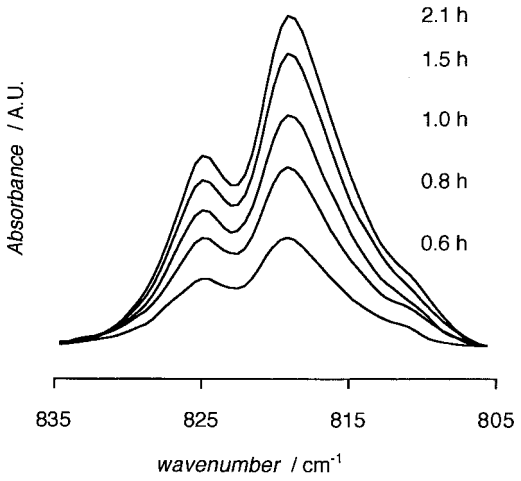

Figure 4. Difference spectra of PPS obtained by subtracting the absorbance measured at the time indicated from that recorded at $t = 0$, in the experiment carried out at the temperature of 98 °C.

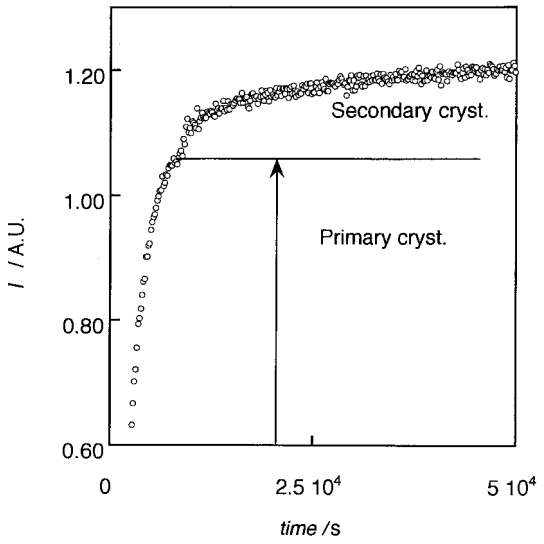

Figure 5. Integral intensity I measured at 98 °C as function of crystallization time.

in-phase and out-phase vibrations, and that of the shoulder at 812 cm^{-1}. Figure 4 shows the evolution of the difference spectrum obtained by subtracting the absorbance measured at t time from that recorded at $t = 0$, in the experiment carried out at the temperature of 98 °C.

As it was anticipated in the introduction of the present paper we have analyzed the crystallization kinetic results of our experiments in terms of the Avrami equation

$$X_p = 1 - \exp(-k\,t^n) \quad (1)$$

X_p is the conversion degree of the primary crystallization process, defined as the ratio between the integral intensity I_t of the difference spectrum bands in the interval 835–805 cm^{-1}, measured I_p at the time t and I_p at t_p, the end of the primary crystallization process. n is the exponent of time in the Avrami equation, depending upon the nucleation mechanism and growth morphology of the crystalline phase. k is the crystallization rate constant.

We have chosen to use the integral intensity of the peak instead of its maximum being the former a more precise estimate for a quantitative analysis.[23] Another reason of our choice is due to the fact that the shape evolution of the IR band is essentially correlated to the increase of the crystalline phase and in a much smaller extent to the effects of the temperature variation on the overall spectrum. These effects in fact may mainly be present in the initial stage of the sample heating, when it reaches the temperature of the isothermal phase transition.

The crystallization experiment was followed for quite a long time and it could not be entirely interpreted by the Avrami law. Except for the $T_c = 90$ °C, the IR analysis showed in a very clear way that at the end of the primary crystallization another process started. In fact the start of a second crystallinity increase could clearly be detected. Figure 5 shows the variation of the I integral obtained from the difference spectrum in the range 805–835 cm^{-1} as function of the crystallization time in the experiment carried out at $T_c = 98$ °C.

As one can see, the beginning of a secondary crystallization process is very clearly detectable.

The I_p value was the intensity measured in correspondence of the beginning of the secondary process (when, as in the Figure, it is clearly appreciable) or in such a way to have the best fit of the Avrami equation for the longest time in the first part of the experimental curve.[24] Figure 6 shows the variation of the conversion degree with time during the isothermal treatment and the theoretical expected Avrami curve for different T_c.

The values of the time t_p measured at the end of primary crystallization, of the rate constant of the primary crystallization process k and of the Avrami exponent n as well as of their standard deviation (σ) for different isothermal crystallization temperature T_c are shown in Table 2.

As one can see, n increases with T_c from 1.4 to 2.1. This trend, reported in other works concerning PPS[7] or other polymers,[25] may be caused by the gradual overlap of more crystallization mechanisms as the crystallization rate increases.

Figure 7 shows the dependence on the crystallization temperature of the relative crystallinity R, corrected for the temperature variation and determined in correspondence of the t_p time at which, in a first approximation, one can consider the ending of the primary crystallization process and the beginning of the secondary one. The R trend, showing the increase of crystallinity with crystalli-

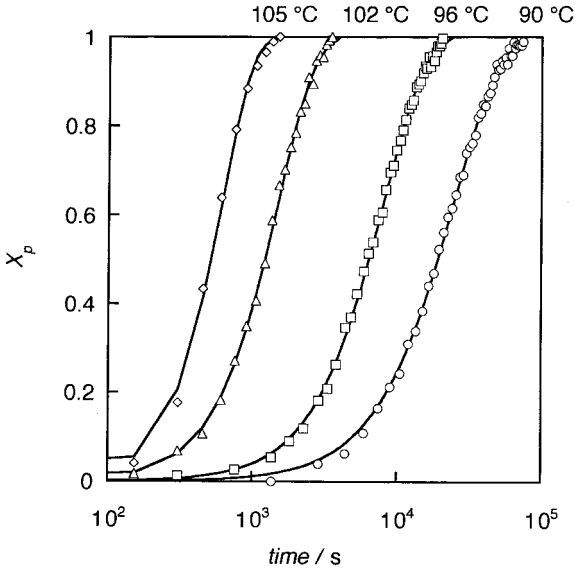

Figure 6. Variation of the conversion degree X_p with time during the isothermal treatment and the theoretical expected Avrami curve for different T_c. For seek of clarity only 30% and 10% of the data for T_c = 96 °C and T_c = 90 °C respectively were reported.

Table 2. Time t_p measured at the end of primary crystallization and crystallization parameters calculated using the Avrami model in IR experiments.

$\frac{T_c}{°C}$	$\frac{t_p}{s}$	$\frac{k}{s^{-n}}$	σ_k	n	σ_n
90	74729	$7.2 \cdot 10^{-7}$	$4 \cdot 10^{-8}$	1.4	0.1
96	21156	$1.3 \cdot 10^{-6}$	$1 \cdot 10^{-7}$	1.5	0.1
98	7915	$3.2 \cdot 10^{-6}$	$4 \cdot 10^{-7}$	1.6	0.1
100	5636	$1.5 \cdot 10^{-5}$	$4 \cdot 10^{-6}$	1.6	0.1
102	3884	$4.3 \cdot 10^{-6}$	$8 \cdot 10^{-7}$	1.7	0.1
104	1447	$4 \cdot 10^{-5}$	$2 \cdot 10^{-5}$	1.7	0.1
105	948	$4 \cdot 10^{-6}$	$1 \cdot 10^{-6}$	2.1	0.1

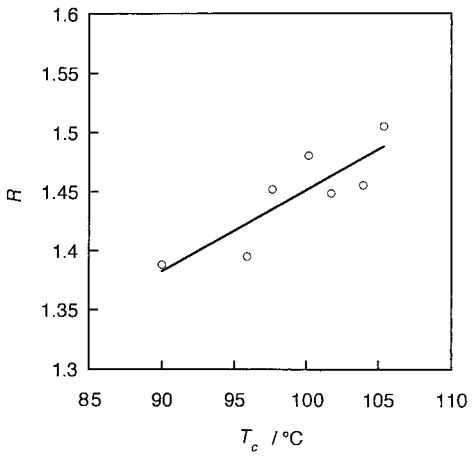

Figure 7. Dependence on T_c of absorbance ratio R = Abs_{1091}/Abs_{1072} recorded at $t = t_p$.

zation temperature, does not indicate that a larger degree of order is reached when the crystallization process is slower, as it happens for the melt crystallization. On the contrary it indicates that at the highest temperature the conditions are met for an higher diffusional capacity of the polymeric chains favoring the crystallinity increase. Such finding agrees with the data reported in the papers of Chung and Cebe,[6] Lu et al.[15] and Cole et al.[18]

EDXD Analysis

Another non-usual technique that we have employed to study the PPS crystallization has been the energy dispersive X-ray diffraction, which rapidly allows the detection of structural changes in the matter. This is possible because the whole energy irradiated by the X-ray source is used instead of a monochromatic radiation. The great advantage of this technique respect with the conventional angular dispersive X-ray diffraction (ADXD) was widely reviewed in ref.,[19] in which a new EDXD method applied to the kinetic of phase transition of inorganic and polymer system was described (EDXD-PT). The qualities of the EDXD, compared with the ADXD technique, may be summarized in:

- reduction in the acquisition time;
- steady apparatus during data collection;
- parallel collection of the spectrum points.

On the other hand a few defects must be noticed:

- complication of experimental data processing;
- need to join various X-ray spectra to reconstruct the whole diffraction pattern;
- decrease in the q resolution.

Unlike the ordinary EDXD measurements that are carried out to obtain the structure factor, in the EDXD applied to phase transition, high resolution and the combination of more diffraction spectra corresponding to various q ranges acquired at different angles is not required and the drawbacks are completely overcome.

Figure 8 shows the EDXD spectra as function of the scattering vector **q** of quenched PPS measured at a temperature of 100 °C before crystallization (A) and after crystallization from the solid amorphous state (B) at T_c = 100 °C for a total crystallization time t = 6600 s as well as their difference B-A (C). The most evident variations are mainly found in the range 1.0–2.5 Å^{-1}. The negative values in the difference spectrum at 1.24 and 1.63 Å^{-1} are due to the sharpening of the peak centered at 1.36 Å^{-1}, which drastically increases during crystallization and shifts to 1.42 Å^{-1}. Analogously in correspondence of q = 1.85 Å^{-1} a shoulder in the amorphous sample spectrum changes in a well defined peak. The spectral changes at highest q values, which imply variation in the distribution of smaller distances, may be considered negligible, although a small positive difference is found between 2.38 and 2.79 Å^{-1}.

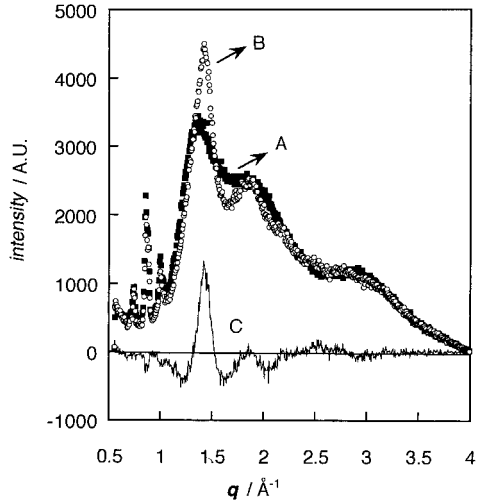

Figure 8. EDXD diffraction spectra of PPS (T_c = 100 °C) measured at 100 °C, t = 0 (A), t = 6600 s (B) and their difference B-A (C).

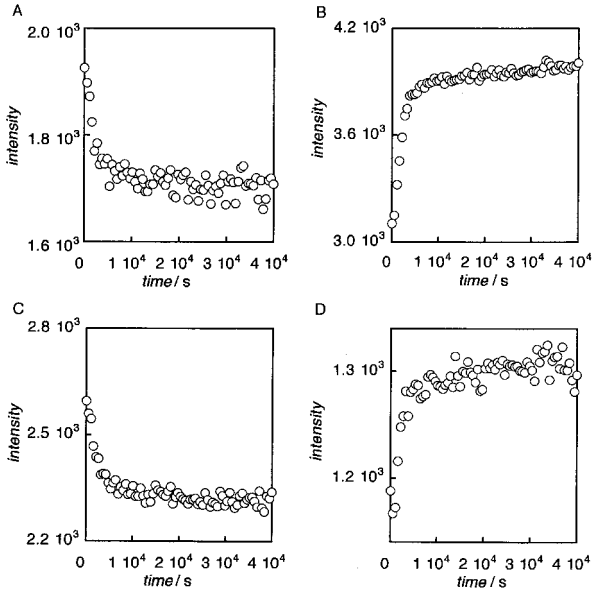

Figure 9. EDXD intensity measured on PPS (T_c = 100 °C) as function of crystallization time in the q regions 1.04–1.34 Å^{-1} (inset A), 1.34–1.52 Å^{-1} (inset B), 1.52–1.67 Å^{-1} (inset C) and 2.38–2.79 Å^{-1} (inset D).

In Figure 9 we show the diffracted X-ray intensity variations measured in correspondence of the aforesaid largest deviations in the difference spectrum, i.e. in the q regions 1.04–1.34, 1.34–1.52, 1.52–1.67, 2.38–2.79 Å^{-1} during the isothermal crystallization experiment carried out at 100 °C.

As it can be seen, the intensity variation measured as function of time for different q intervals is always described by the same kinetic law except for the sign. This would mean that the structural variations observed in the 1.04–2.79 Å^{-1} q region arising during the crystallization, all correspond to the same transformation process. Also the EDXD technique enlightens a secondary crystallization process (see Figure 10A) as it was shown by the infrared analysis, although the noise of the experimental points is higher than that found in the IR experiments. In fact a stepwise increase of crystallinity is detectable in the diffracted intensity after the first rapid crystallinity growth (primary process) measured as function of time.

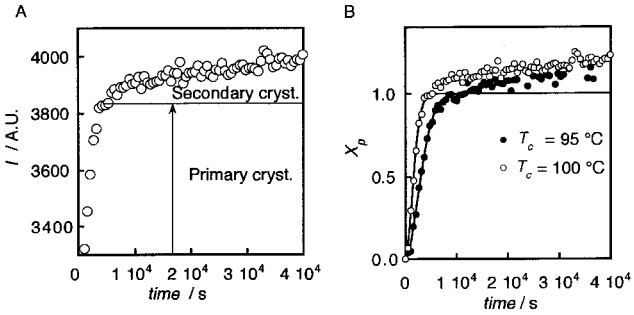

Figure 10. EDXD analysis. (A) EDXD intensity measured in the q region 1.34–1.52 Å^{-1} at T_c = 100 °C and (B) conversion degree X_p for T_c = 95 and 100 °C as function of the crystallization time (the solid lines show the theoretical expected Avrami curve).

As in the case of the infrared analysis, the EDXD experimental data have been interpreted by means of the Avrami Equation, so deriving the rate constant k and the Avrami exponent n from the degree of conversion X_p defined as

$$X_p = (I - I_0)/(I_p - I_0) \quad (2)$$

in which I is the integral diffracted intensity measured in the q region 1.34–1.52 Å^{-1} at the generic time t, I_0 is the one measured at t = 0 and I_p that at $t = t_p$ (the ending of the primary process). Figure 10B shows how X_p varies as function of crystallization time for two different T_c (95 and 100 °C).

The derived kinetic parameters are reported in Table 3.

Table 3. Time t_p measured at the end of primary crystallization and crystallization parameters calculated using Avrami model in EDXD experiments.

T_c / °C	t_p / s	k / s^{-n}	σ_k	n	σ_n
95	11667	$3 \cdot 10^{-7}$	$1 \cdot 10^{-7}$	1.8	0.1
100	5336	$1.1 \cdot 10^{-6}$	$5 \cdot 10^{-7}$	1.8	0.1

DSC Analysis

In order to follow the whole isothermal cold-crystallization process by means of the DSC technique and then acquire data suitable for the Avrami analysis the temperature range that might be explored was necessary small:

108–112 °C. At higher temperature, in fact, the crystallization process is so rapid that it takes place before temperature stabilization, while at lower temperature, because of the instrumental sensibility, it is not possible to measure the low heat flow involved in the transformation. DSC evidences just a single exothermal peak for the isothermal transformation of PPS, in contrast with the two other techniques that we have already discussed. Indeed, after the primary process of crystallization, a flat and horizontal baseline of the DSC trace does not reveal an observable secondary process.

The crystallization was analyzed by applying the Avrami equation to the degree of polymer transformation X_c, defined as the ratio between the partial peak area at time t and the total exothermic peak area of the DSC trace, that is:

$$X_c = \frac{\int_0^t (dH/dt)dt}{\int_0^\infty (dH/dt)dt} \quad (3)$$

where dH/dt is the heat flow recorded during crystallization. In Figure 11 the crystallization process at 112 °C is reported.

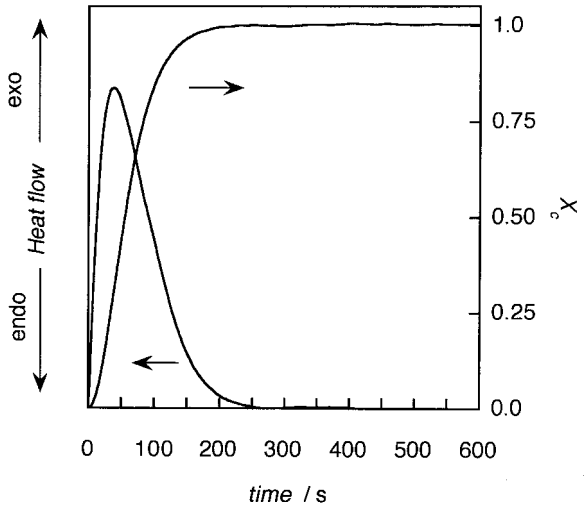

Figure 11. DSC isothermal crystallization curve of PPS (T_c = 112 °C) and the correspondent X_c variation as function of crystallization time.

The kinetic parameters n and k found are listed in Table 4. It must be pointed out that the scattering of the data and the particularly low n value found for the crystallization temperature of 108 and 110 °C may be caused by the small heat flow and in the detection of the transformation starting point. The above mentioned problems may induce to underestimate the n value.

Table 4. Crystallization parameters calculated using the Avrami model in DSC experiments.

$\frac{T_c}{°C}$	$\frac{k}{s^{-n}}$	σ_k	n	σ_n
108	$1.64 \cdot 10^{-3}$	$5 \cdot 10^{-5}$	1.3	0.1
110	$5.6 \cdot 10^{-3}$	$3 \cdot 10^{-4}$	1.3	0.1
112	$1.25 \cdot 10^{-3}$	$7 \cdot 10^{-5}$	1.6	0.1

Discussion of the Primary Crystallization

Although the Avrami equation is widely discussed and often its kinetic parameters loose the physical meaning attributed by the theory, nevertheless it is still generally adopted for both the treatment of the experimental data and in the formulation of new theories about the crystallization kinetics of polymers. This is due to the artlessness of the equation which implies just two parameters and to the possibility of easy comparability of the results obtained in different experimental conditions on the same polymeric material. However, all the people concerned with the interpolation of the experimental data by means of the Avrami equation have surely been troubled for the different results obtained by the different computational strategies employed on data sets which are quite often not very clean, as those relative to the beginning and to the end of the transformation. Not always such a difficulty may be surmounted, as in the case of particularly slow or rapid transformations involving small heat flows. For this reason we have decided to look at the crystallization phenomenon by following it through three different properties of the polymer: the changes in the IR absorptions due to roto-vibrations movements (FT-IR), the thermodynamic properties of the material, i.e., the heat flow involved in the phase transition (DSC), and the structural modifications (EDXD). The above mentioned techniques cover a sufficiently large range of time/temperature so allowing a quite detailed kinetic analysis of the collected data by means of the Avrami equation.

All the kinetic elaboration were carried out considering the PPS composed by two phases: the crystalline and amorphous one.

The Figure 12 A shows how the observed t_{peak} (at which the highest crystallization rate is reached) value varies as a function of the T_c. All the data, collected by means of the different techniques employed and directly obtained from the experimental data, without any subsequent mathematical treatment, may be interpolated by the same curve over the overall T_c range explored.

These data, in our case, are slightly different from those reported by Chung and Cebe[6] for their DSC cold-crystallization experiments on PPS. Such a small difference could be attributed to the probably different quenching conditions. The results of our analysis are summarized in Table 5, where the derived n and k parameters are reported. It is worth noticing that the isothermal crystallization process was observed up to 90 °C, which is the temperature more often quoted as typical of the glass transition phenomena for this polymer (we have however

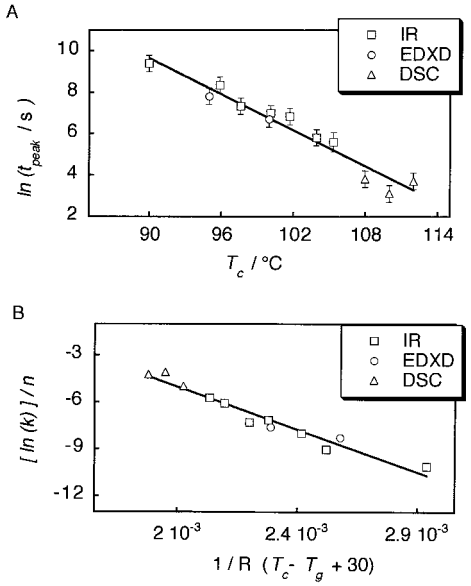

Figure 12. (A) Time corresponding to the maximum crystallization rate t_{peak} as function of T_c and (B) dependence of (ln k)/n as function of $1/[R(T_c - T_g + 30)]$ according to Hoffmann theoretical model, as measured by means of IR, EDXD and DSC.

Table 5. Crystallization parameters calculated using the Avrami model employing the three techniques.

T_c / °C		k / s^{-n}	σ_k	n	σ_n	t_{peak} / s
90	IR	$7.2 \cdot 10^{-7}$	$4 \cdot 10^{-8}$	1.4	0.1	11 842
96	IR	$1.3 \cdot 10^{-6}$	$1 \cdot 10^{-7}$	1.5	0.1	4 150
98	IR	$3.2 \cdot 10^{-6}$	$4 \cdot 10^{-7}$	1.6	0.1	1 509
100	IR	$1.5 \cdot 10^{-5}$	$4 \cdot 10^{-6}$	1.6	0.1	664
102	IR	$4.3 \cdot 10^{-6}$	$8 \cdot 10^{-7}$	1.7	0.1	924
104	IR	$4 \cdot 10^{-5}$	$2 \cdot 10^{-5}$	1.7	0.1	200
105	IR	$4 \cdot 10^{-6}$	$1 \cdot 10^{-6}$	2.1	0.1	391
95	EDXD	$3 \cdot 10^{-7}$	$1 \cdot 10^{-7}$	1.8	0.1	2426
100	EDXD	$1.1 \cdot 10^{-6}$	$5 \cdot 10^{-7}$	1.8	0.1	807
108	DSC	$1.64 \cdot 10^{-3}$	$5 \cdot 10^{-5}$	1.3	0.1	45
110	DSC	$5.6 \cdot 10^{-3}$	$3 \cdot 10^{-4}$	1.3	0.1	22
112	DSC	$1.25 \cdot 10^{-3}$	$7 \cdot 10^{-5}$	1.6	0.1	40

already demonstrated[1] how the PPS T_g should be located below 70 °C).

The average value obtained for the n Avrami coefficient is 1.6, although the Avrami theory does not consider fractional values for this parameter. However Wunderlich, in his book on the Physical Properties of Polymers,[26] proposes $n = 3/2$ to describe the isothermal heterogeneous crystallization wholly governed by transport process and $n = 5/2$ for the homogeneous one. Banks and Sharples[27] and Velisaris and Seferis[28] have made the hypothesis that fractional values could be due to the overlapping of a plurality of crystallization mechanisms. Other researchers have proposed that such fractional values could be attributed to the overlapping of the primary crystallization defined by an integer $n > 1$ and the secondary one defined by $n = 1$, being the secondary process intra-spherulitic[29] or intra and inter-spherulitic.[10]

The application of the aforementioned theories to our data regarding the primary process by the assumption of an integer value of n did not give a satisfactory fitting of the experimental data. While for the melt crystallization the literature furnishes n values ranging between 1.9 and 3.1, those found by us for our cold-crystallization experiments were on average a factor of 1 lower. This could be due to the heterogeneous mechanism involved in the latter case, where the substantially amorphous bulk of the material contains a large number of crystalline nuclei. They are characterized by a short range order not able to produce Bragg reflections in the X-ray diffraction experiment, as it was hypothesised by Chung and Cebe[6] in their analysis of t_{peak} data.

Moreover, as stressed in the following discussion, the quenching procedure does not secure the perfect reproducibility, what may influences the concentration of these nuclei and then the polymer crystallization rate. This is reflected on the scattering of the k values shown in Table 5. The data dispersion greatly decreases if the normalized kinetic constants $k^{1/n}$ is analyzed, being taken into account the possible crystallization mechanism change/overlapping or, as in the case of DSC experiments, the difficulty in detecting of the transformation starting point.

Influence of T_c on the Crystallization Rate

The spherulitic radial growth rate G depends on the T_c as stated by the well known Hoffmann equation[30]

$$G = G_0 \exp[-U^*/R(T_c - T_\infty)] \exp[-K_g/T_c(T_m^0 - T_c)f] \quad (4)$$

where G_0 is a pre-exponential term, independent on temperature.

In the first exponential, representing the diffusional contribution to the growth rate, U^* is the activation energy needed for the chains movement and T_∞ represents the temperature at which they are motionless. U^* and T_∞ obtained by the Williams-Landel-Ferry equation (WLF) through viscoelastic measurements give $U^* = 17.24$ kJ · mol^{-1} and $T_\infty = T_g - 51.6$ K, where T_g is the glass transition temperature (Adam and Gibbs[31] state that it has to be measured in quasi-static experiments). For the type of application we are discussing, however, the values $U^* = 6.28$ kJ · mol^{-1} and $T_\infty = T_g - 30$ K are preferred.[30]

In the second exponential $K_g = n\, b_0\, \sigma\, \sigma_e / \Delta h_f\, R$, where n is related to the growth mechanism of the molecular layer adsorbed on the lamellar surface ($n = 4$ in regime I and III, $n = 2$ in regime II), σ and σ_e are lateral surface and fold surface free energy, b_0 is the layer molecular thickness, Δh_f is the enthalpy of fusion and R the Boltz-

mann's constant, T^0_m is the equilibrium melting temperature and f is a term which takes into account the temperature dependence of Δh_f, $f = 2T_c/(T^0_m + T_c)$.

Generally the bulk crystallization rate, normalized for the Avrami exponent n, may be assumed proportional to G

$$G \propto k^{1/n} \tag{5}$$

Moreover for the low temperature of a cold-crystallization experiment the second exponential of the Hoffmann equation may be considered as a constant and included in the pre-exponential term. Then the crystallization rate dependence on T_c becomes

$$(\ln k)/n = \ln(k_0) - [U^*/\mathrm{R}\,(T_c - T_\infty)] \tag{6}$$

Figure 12B shows the dependence of $(\ln k)/n$ on $1/\mathrm{R}(T_c - T_\infty)$, having assumed for T_∞ the equation $T_\infty = T_g - 30$ K and $T_g = 78\,^\circ$C = 351 K.

The value obtained for U^* is equal to the theoretical one $U^* = 6.28$ kJ · mol^{-1}. Moreover it is worth of notice that the $T_g = 78\,^\circ$C value used by us, although 7–8 °C lower than that usually found in DSC measurements performed at an heating rate of 10 or 20 °C · min^{-1}, is experimentally accessible, as it was demonstrated in a previous study accomplished by us by employing heating rate consistently lower (0.05–1 °C · min^{-1}) and looking at the glass transition phenomenon by FT-IR and EDXD analysis.[1] On the contrary, if one imposes $T_g = 84\,^\circ$C a lower value of U^* is obtained ($U^* = 5.0$ kJ · mol^{-1}).

By applying the equation $T_\infty = T_g - 51.6$ K with $T_g = 67\,^\circ$C the other predicted value of $U^* = 17.24$ kJ · mol^{-1} is obtained. Such a small value of T_g may be considered reasonable too if one looks how our T_g data extrapolates at the lowest heating rate.

In their work Lovinger et al.[3] have obtained on PPS Ryton V-1 $U^* = 5.86$ kJ · mol^{-1} by imposing $T_g = 84\,^\circ$C and $T_\infty = T_g - 30$ K. The application of the WLF derived parameters does not give a good fit of the experimental data in the low-temperature region.

As far as the kinetic rate constant k is concerned it is worth to remember that, in the case of the predetermined nucleation (heterogeneous crystallization), it depends on the spherulitic linear growth rate G and on the number of the crystallization nuclei which are present in the quenched sample as well as on their dimensional distribution. This could explain the dispersion of the $(\ln k)/n$ data of Figure 12B, being the quenching procedure particularly delicate for polymers characterized by high crystallization rate.

Secondary Crystallization

In a previous paper[1] on the PPS glass transition we anticipated that the infrared spectrum of the polymer showed a marked variation on intensity and shape of some absorption bands in correspondence of the crystallization process occurring above T_g. Such a first discontinuity was followed by a second upraise, which was assigned to the beginning of a secondary crystallization process. Such a phenomenon had already been observed, although not discussed, by Menczel and Collins[8] in their DSC experiments on quenched PPS. These experiments, performed at an heating rate of 10 K · min^{-1}, showed a double crystallization endothermal peak. Such evidence, obtained in non-isothermal conditions, has also been found in our laboratory and will be the object of a forthcoming paper.

In the isothermal conditions of the experiments we are discussing here, except for the lower crystallization temperature employed, we have found a stepwise crystallinity increase at the ending of the primary process described by the Avrami equation (see Figure 5 and 10A). Such behavior was described in 1960 by Rybnikar,[32] who found the apparent start of the secondary crystallization process at a time nearly double that of the half-crystallization time of the primary process ($t_{1/2}$). This author[33] considered the two processes as distinct and found a value of the Avrami $n = 1$ for the second one. Moreover he enlightened that the crystallinity increase with time was not stopped at the ending of the secondary process and proposed that the overall crystallization could be described by three different processes.

Although our EDXD data are more scattered than the IR ones, which very clearly show the beginning of the secondary process, we can say that our finding on the apparent beginning time of the secondary process t_s confirms those of Rybnikar ($t_s \geq 2\,t_{1/2}$). We have followed the overall crystallization of PPS for $t_s = 10\,t_{1/2}$, at the end of which we have calculated a 2–3% contribution of secondary process to the total crystallinity. Figure 13A shows how the growing parameter R ($R = \mathrm{Abs}_{1091}/\mathrm{Abs}_{1072}$) varies with $\ln(t - t_s)$.

Except for the lower crystallization temperature employed (90 °C for the IR experiments), for which the crystallization was followed for $t < 10\,t_{1/2}$ and whose data are not included in the Figure, a linear dependence of R on $\ln(t - t_s)$ may be assumed.

The angular coefficient of these straight lines is proportional to the rate of increase of the polymer crystallinity due to the secondary process. Figure 13B shows the dependence of such a parameter on the crystallization temperature.

The secondary crystallization has been interpreted in different ways in different theoretical frameworks:

- a continuous perfectioning process of the crystalline phase produced in the primary process;[33]
- a further transformation of the amorphous phase in the crystalline one, but made more difficult because of loops and entanglements which may be removed as time goes on;[34]

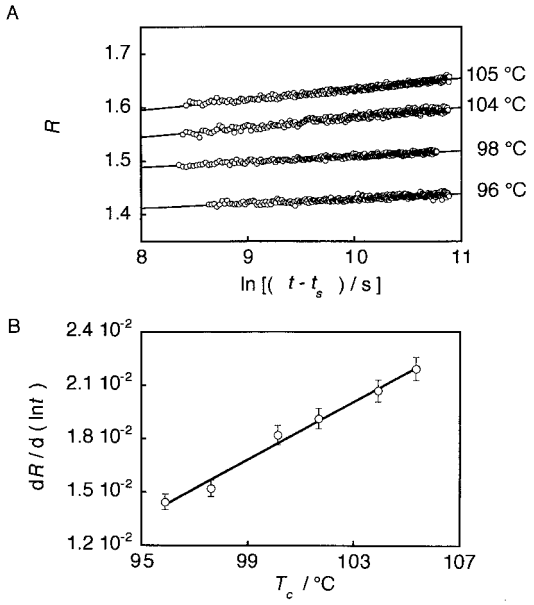

Figure 13. (A) Absorbance ratio R as function of ln $(t-t_s)$ for different T_c during secondary crystallization process and (B) dR/d(ln t) value as function of crystallization temperature T_c.

- an order making process of originally segregated smaller molecular weight fractions.[29]

We have attempted to analyze the secondary crystallization process by means of the theory proposed by Ravindranath and Jog.[10] Such a theory was derived from the original works of Rybnikar[32, 33] and Hillier[29] and was intended to explain the observed deviations (fractional values of n) from the Avrami law during the primary melt-crystallization of PPS. Such a theory considers the overall crystallization process as the summation of a primary process described by the Avrami law and a secondary one, which follows an Avrami-like equation with $n = 1$ starting at a time τ, transforming the amorphous phase in an ordered one within the inter- and intraspherulitic yet formed domains. Its Equation may be written as

$$X_c = X_p\,[1-\exp(-k_p\,t^n)] + X_s\,[1-\exp\,(-k_s\,(t-\tau)] \qquad (7)$$

in which X_p and X_s are the fractions of the amorphous polymer crystallized at infinite time in a primary and a secondary process respectively, and k_p and k_s are the corresponding rate constants.

Although such an equation contains a larger number of parameters to be optimized compared to the simple Avrami law, not any hypothesis is needed on the ending of the primary process and the beginning of the secondary one and allows us to follow the overall crystallization phenomenon for a considerably longer time.

While an integer value of the n Avrami exponent ($n = 2$ in the case of cold-crystallization) does not give a good fit of the experimental data, if one lets n to be optimized a satisfactory agreement between the observed and calculated values is obtained by the use of the above mentioned equation. Table 6 shows the k_p, n, k_s and τ values obtained by using Equation (7).

Table 6. Crystallization parameters calculated using Equation (7).

T_c / °C		k_p / s^{-n}	n	k_s / s^{-1}	τ / s
90	IR	$2 \cdot 10^{-7}$	1.5	$2.0 \cdot 10^{-5}$	9023
96	IR	$6 \cdot 10^{-7}$	1.6	$4.6 \cdot 10^{-5}$	8024
98	IR	$5 \cdot 10^{-6}$	1.5	$1.0 \cdot 10^{-4}$	7904
100	IR	$1.0 \cdot 10^{-4}$	1.3	$2.4 \cdot 10^{-5}$	2279
102	IR	$2.4 \cdot 10^{-5}$	1.5	$4.4 \cdot 10^{-5}$	3377
104	IR	$4.1 \cdot 10^{-4}$	1.3	$7.5 \cdot 10^{-5}$	1025
105	IR	$1.6 \cdot 10^{-5}$	1.7	$4.8 \cdot 10^{-5}$	1240
95	EDXD	$5 \cdot 10^{-8}$	2.0	$6 \cdot 10^{-5}$	8569
100	EDXD	$4 \cdot 10^{-6}$	1.6	$5 \cdot 10^{-5}$	4401

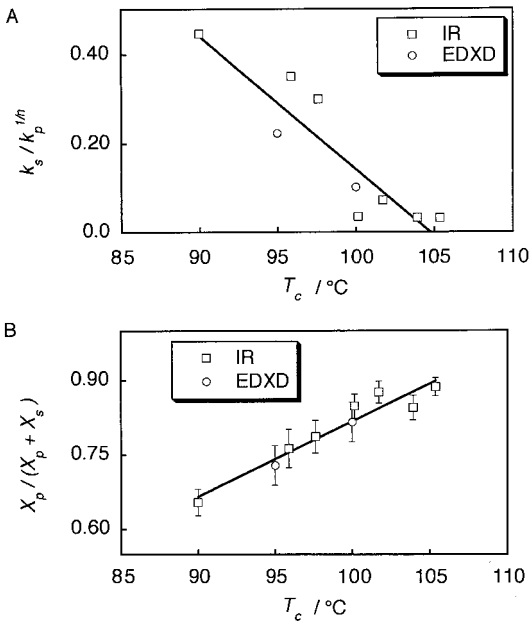

Figure 14. (A) Rate constant ratio of primary and secondary crystallization process and (B) primary process crystallinity fraction calculated according to Equation (7) as function of T_c, as measured by means of IR and EDXD.

Figure 14A shows how the ratio of the rate constants of the primary and secondary process varies as function of the crystallization temperature.

As it may be seen the primary process is much more influenced by T_c than the secondary, whose rate remains practically constant over the temperature range that we have explored.

Figure 14B shows the dependence on the T_c of the primary process crystallinity fraction. It must be stressed that these values were obtained by applying Equation (7), that is by extrapolating the experimental data to the end

of the transformation at $t = \infty$, and are not to be correlated with the extent of the secondary crystallization derivable from Figure 2 and 10, in which the processes were followed up to 15 and 10 h.

The higher degree of crystallinity reached increasing T_c at the end of the primary process, and the simultaneous increase of the rigid amorphous phase adjacent to the ordered phase, limits the diffusion of the amorphous segments which result to be constrained. This does not allow the increase of the secondary process rate. Indeed Figure 14B shows that the crystallinity is mainly due to the primary process, reaching 90% at 105 °C. The low value for the secondary process explains why it is so difficult to detect it in DSC experiments, where higher crystallization temperature must be employed.

However it must be noticed that the experimental techniques that were used in the present work do not allow to hypothesize the mechanism of the secondary process, lacking the morphological evidences needed on the long range order of the material, as it was underlined by Wunderlich.[26]

Conclusions

The primary cold-crystallization process of PPS is defined by an n Avrami exponent definitely fractional ($n = 1.4–2.1$) which increases with temperature as does the velocity constant k, whose value is of the 10^{-6} order of magnitude, and the reached relative crystallinity. This clearly shows the role of diffusion in this type of crystallization, how it is reasonable to expect. It must be noticed the fact that the n value found by us is very near to the $n = 3/2$ proposed by Wunderlich[26] for transport process controlled crystallization. This probably is not always met because of the different residual crystallinity of the samples, being the quenching technique unable to give the totally amorphous state and very delicate in ensuring the perfect reproducibility of the sample production. Another explanation may be found in the possible overlapping of different crystallization mechanism at the higher T_c. As far as the U^* activation energy needed to enliven the movement of the chains frozen in the disordered state is concerned we have obtained the Hoffman[30] predicted value of 6.28 kJ · mol^{-1} by assuming $T_\infty = T_g - 30$ K and $T_g = 78$ °C, a value in very good agreement with that found by us[1] and well below the 84 °C used by Lovinger.[3] Moreover also our attempts to fit the WLF U^* and T_∞ figures have shown that just employing a very low value (67 °C) for T_g and $T_\infty = T_g - 51.6$ K the theoretical 17.24 kJ · mol^{-1} for the activation energy may be obtained, confirming the reliability of the lower T_g figure found and used by us.

As far as the secondary crystallization is concerned we have been able to enlighten such a process which resulted to be very well described by the Ravindranath and Jog[10] theory, confirming the values obtained by us for the n Avrami exponent of the primary process. It indicates that its velocity constant is practically unaffected by the crystallization temperature which, on the contrary, shows its influence in determining the degree of crystallinity reached at the end of the primary process. This is reflected in a limitation of the chain segments diffusion in the amorphous inter- and intra-spherulitic domains. They result to be constrained and not able to increase the secondary process rate. However the lack of morphological information regarding the long range order reached by our samples does not allow us to make reliable hypothesis regarding the mechanism of the secondary crystallization. Our finding confirm those of Rybnikar[33] concerning the apparent starting time of the secondary crystallization, showing that it is always equal or greater than the double of the half-crystallization time of the primary one. The contribution of the secondary process to the total crystallinity reached by our samples was in the range of 2–3%, although it must be noticed that we could not observe the end of such a process after 24 h.

Acknowledgement: We wish to thank *MURST (Ricerche di Ateneo)* for financial support.

Received: November 21, 2000

[1] R. Caminiti, L. D'Ilario, A. Martinelli, A. Piozzi, C. Sadun, *Macromolecules* **1997**, *30*, 7970.
[2] J. P. Jog, V. M. Nadkarni, *J. Appl. Polym. Sci.* **1985**, *30*, 997.
[3] A. J. Lovinger, D. D. Davis, F. J. Jr Padden, *Polymer* **1985**, *26*, 1595.
[4] L. C. Lopez, G. L. Wilkes, *Polymer* **1988**, *29*, 106.
[5] L. C. Lopez, G. L. Wilkes, J. F. Geibel, *Polymer* **1989**, *30*, 147.
[6] J. S. Chung, P. Cebe, *J. Polym. Sci., Part B: Polym. Phys.* **1992**, *30*, 163.
[7] A. Maffezzuoli, J. M. Kenny, L. Nicolais, *Thermochim. Acta* **1992**, *199*, 133.
[8] J. D. Menczel, G. L. Collins, *Polym. Eng. Sci.* **1992**, *32*, 1264.
[9] A. Maffezzuoli, J. M. Kenny, L. Nicolais, *Thermochim. Acta* **1993**, *227*, 83.
[10] K. Ravindranath, J. P. Jog, *J. Appl. Polym. Sci.* **1993**, *49*, 1395.
[11] C. Auer, G. Kalinka, Th. Krause, G. Hinrichsen, *J. Appl. Polym. Sci.* **1994**, *51*, 407.
[12] E. M. Woo, J. M. Chen, *J. Polym. Sci., Part B: Polym. Phys.* **1995**, *33*, 1985.
[13] K. Könnecke, *J. Macromol. Sci. Phys.* **1994**, *B33*, 37.
[14] S. S. Wu, D. S. Kalika, R. R. Lamonte, S. J. Makhija, *J. Macromol. Sci. Phys.* **1996**, *B35*, 157.
[15] S. X. Lu, P. Cebe, M. Capel, *Macromolecules* **1997**, *30*, 6243.

[16] P. Huo, P. Cebe, *J. Polym. Sci., Part B: Polym. Phys.* **1992**, *30*, 1239.
[17] J. A. Ferrara, J. C. Seferis, C. H. Sheppard, *J. Thermal. Anal.* **1994**, *42*, 467.
[18] K. C. Cole, D. Noel, J.-J. Hechler, *J. Appl. Polym. Sci.* **1990**, *39*, 1887.
[19] R. Caminiti, V. Rossi Albertini, *Int. Rev. Phys. Chem.* **1999**, *18*, 263.
[20] D. J. Brady, *J. Appl. Polym. Sci.* **1976**, *20*, 2541.
[21] P. Piaggio, C. Cuniberti, G. Dellepiane, E. Campani, G. Gorini, G. Masetti, M. Novi, G. Petrillo, *Spectrochim. Acta Part A* **1989**, *45*, 347.
[22] D. A. Zimmerman, J. L. Koenig, H. Ishida, *Spectrochim. Acta Part A* **1995**, *51*, 2397.
[23] H. Hagemann, R. G. Snyder, A. J. Peacock, L. Mandelkern, *Macromolecules* **1989**, *22*, 3600.
[24] A. Sharples, "*Introduction to Polymer Crystallization*", Edward Arnold, London 1966.
[25] E. Urbanovici, H. A. Schneider, H. J. Cantow, *J. Polym. Sci., Part B: Polym. Phys.* **1997**, *35*, 359.
[26] B. Wunderlich, "*Macromolecular Physics*. *Crystal Nucleation, Growth, Annealing*", Vol. 2, Academic Press, New York 1976.
[27] W. Banks, A. Sharples, *J. Polym. Sci., Part A* **1964**, *2*, 4059.
[28] C. N. Velisaris, J. C. Seferis, *Polym. Eng. Sci.* **1986**, *26*, 1574.
[29] H. I. Hillier, *J. Polym. Sci., Part A* **1965**, *3*, 3067.
[30] J. D. Hoffman, G. T. Davis, J. I. Jr Lauritzen, in: "*Treatise on Solid-State Chemistry*", Vol. 3, N. B. Hannay, Ed., Plenum Press, New York 1976, Chapter 7.
[31] G. Adam, J. H. Gibbs, *J. Chem. Phys.* **1965**, *43*, 139.
[32] F. Rybnikar, *J. Polym. Sci*. **1960**, *44*, 517.
[33] F. Rybnikar, *J. Polym. Sci., Part A* **1963**, *1*, 2031.
[34] H. G. Zachmann, H. A. Stuart, *Makromol. Chem.* **1960**, *41*, 131.